THE UNIVERSITY of EDINBURGH

Edinburgh Research Explorer

A Multi-CAP Visible-Light Communications System With 4.85-b/s/Hz Spectral Efficiency

Citation for published version:
Haigh, PA, Burton, A, Werfli, K, Minh, HL, Bentley, E, Chvojka, P, Popoola, WO, Papakonstantinou, I & Zvanovec, S 2015, 'A Multi-CAP Visible-Light Communications System With 4.85-b/s/Hz Spectral Efficiency', *IEEE Journal on Selected Areas in Communications*, vol. 33, no. 9, pp. 1771-1779. https://doi.org/10.1109/JSAC.2015.2433053

Digital Object Identifier (DOI):
10.1109/JSAC.2015.2433053

Link:
Link to publication record in Edinburgh Research Explorer

Document Version:
Peer reviewed version

Published In:
IEEE Journal on Selected Areas in Communications

General rights
Copyright for the publications made accessible via the Edinburgh Research Explorer is retained by the author(s) and / or other copyright owners and it is a condition of accessing these publications that users recognise and abide by the legal requirements associated with these rights.

Take down policy
The University of Edinburgh has made every reasonable effort to ensure that Edinburgh Research Explorer content complies with UK legislation. If you believe that the public display of this file breaches copyright please contact openaccess@ed.ac.uk providing details, and we will remove access to the work immediately and investigate your claim.

Download date: 29. Apr. 2024

A Multi-CAP Visible Light Communications System with 4.85 b/s/Hz Spectral Efficiency

Paul Anthony Haigh, Andrew Burton, Khald Werfli, Hoa Le Minh, Edward Bentley, Petr Chvojka, Wasiu O. Popoola, Ioannis Papakonstantinou and Stanislav Zvanovec

***Abstract*—In this paper we experimentally demonstrate a multiband carrier-less amplitude and phase modulation format for the first time in VLC. We split a conventional carrier-less amplitude and phase modulated signal into m subcarriers in order to protect from the attenuation experienced at high frequencies in low-pass VLC systems. We investigate the relationship between throughput/spectral efficiency and m, where $m = \{10, 8, 6, 4, 2, 1\}$ subcarriers over a fixed total signal bandwidth of 6.5 MHz. We show that transmission speeds (spectral efficiencies) of 31.53 (4.85), 30.88 (4.75), 25.40 (3.90), 23.65 (3.60), 15.78 (2.40), 9.04 (1.40) Mb/s (b/s/Hz) can be achieved for the listed values of m, respectively.**

***Index Terms*—Bit error rate, equalizers, light emitting diodes, visible light communications**

I. Introduction

SEVERE bandwidth limitation introduced by light-emitting diodes (LEDs) is the major bottleneck to high capacity visible light communications (VLC) systems. The vast majority of VLC links employ blue gallium nitride (GaN) LEDs with cerium-doped yttrium aluminium garnet (Ce:YAG) yellowish phosphor wavelength converters to achieve white light [1–3]. This is an inexpensive and simple solution to providing a high level of illumination and also data communications simultaneously. On the other hand, the major problem is that optimized GaN LEDs can have bandwidths in the GHz region [4], while the Ce:YAG phosphor is limited to the low MHz region, with values reported in the literature ranging up to 3 MHz [5], [6]. To overcome this bandwidth limitation there have been suggestions to use optical bandpass filters to isolate the fast blue component and reject the slow yellowish component, with remarkable gains up to 26 MHz [5], [6]. Using optical filters is a suboptimal solution because they introduce a severe reduction in the signal power (up to 50% [7]), and hence a hugely reduced signal-to-noise ratio (SNR). Furthermore, in [3] it was reported that with the appropriate digital signal processing and equalization at the receiver, a higher transmission speed could be supported with the whole spectra of white light (170 Mb/s) in comparison to the blue filter (150 Mb/s) due to the reduction in SNR. Thus it is desirable to avoid the use of the blue filter, where possible. Aside from using equalizers at the receiver, the most commonly proposed technique to improve the transmission speed of white phosphor based VLC systems is the use of modulation formats that offer high spectral efficiency, such as orthogonal frequency division multiplexing (OFDM), which has shown remarkable capacity gains in the literature up to ∼1.5 Gb/s using a single Ce:YAG phosphor converted GaN LED [8]. In order to achieve such a transmission speed, additional signal processing techniques such as the adaptive bit- and power-loading were introduced [9] to compensate for the attenuation of the high frequencies.

In recent times, OFDM is beginning to decline in popularity in VLC systems with the re-emergence of carrier-less amplitude and phase modulation (CAP), which has been experimentally shown to outperform OFDM in terms of transmission speed when using the same link [10], offering a lower bit error rate (BER) and higher throughput of 1.32 Gb/s using CAP and 1.08 Gb/s using OFDM in the best case. Thus CAP is deserving of further attention for research in VLC systems both for this reason and also because it has several other advantages over OFDM. Considering that CAP is a passband modulation format just as in OFDM, one must consider the generation of the carrier frequencies and the complexity it introduces to the system. The most important advantage of CAP over OFDM is that there is no (inverse) fast Fourier transform, while OFDM requires one at the transmitter and one at the receiver. This means that the computational complexity is significantly reduced and real time implementation is more straightforward. It should be noted that in comparison to the simplest scheme; an unequalised on-off keying (OOK) link, the computational complexity is generally increased. The carrier frequencies in CAP are generated by carefully designing the impulse responses of finite impulse response (FIR) filters, which can either be analogue or digital [11]. Digital FIR filters are proposed as the preferred type, being generally cheap, easily reconfigurable, integrated and simple to program.

CAP also provides an advantage over single carrier modulation formats such as quadrature amplitude modulation (QAM) which requires a local oscillator at both the transmitter and receiver. The dominant noise source present in CAP VLC systems is additive white Gaussian noise (AWGN) introduced by the receiver electronics, consistent with other VLC systems

Manuscript received May 28th, 2014, revised October 27th, 2014.

P. A. Haigh is with the Faculty of Engineering, University of Bristol, Bristol, BS8 1TR, UK

A. Burton, K. Werfli, H. Le Minh and E. Bentley are with the Faculty of Engineering and Environment, Northumbria University NE1 8ST, UK

P. Chvojka and S. Zvanovec are with the Department of Electromagnetic Field, Czech Technical University in Prague, 2 Technicka, 16627 Prague, Czech Republic

W. O. Popoola is with the Institute for Digital Communications, School of Engineering, University of Edinburgh, EH9 3JL, UK

I. Papakonstatniou the Department of Electrical and Electronic Engineering, University College London, WC1E 6BT, UK

e-mail: paul.anthony.haigh@ieee.org; {andrew.burton; khald.werfli; hoa.le-minh; edward.bentley}@northumbria.ac.uk; {chvojpe8; xzvanove}@fel.cvut.cz; w.popoola@ed.ac.uk; i.papakonstantinou@ucl.ac.uk

[12].

VLC systems are highly bandlimited, as mentioned and can be modelled as a first order low pass filter [1]. Therefore frequencies outside the 3 dB modulation bandwidth will experience an attenuation of 20 dB/decade, and thus to gain any sufficient gain from a wideband modulation format such as CAP (or OFDM/QAM) frequency domain equalizers such as analogue high pass filters [1], [13] have generally been considered, with post-equalizers at the receiver consistently showing the best performance in the literature [1], [14]. Much as with optical filters, high pass filters in the receiver electronics introduce a significant power penalty due to power dissipation in the discrete components, causing the overall SNR to drop at low frequencies inside the modulation bandwidth. This is a substantial disadvantage when considering multi-carrier systems, where a high number of bits-per-symbol can be selected at these frequencies, thus improving the spectral efficiency. However, traditional CAP is not a multi-carrier system and this technique cannot be applied. In [15] a multi-carrier CAP system is proposed for short-haul optical fibre links. The proposed multi-CAP system (m-CAP, where m is the number of subcarriers) is compared with a traditional single carrier CAP system over 15 km of standard single mode fibre with a 25 GHz externally modulated as the transmitter. The multi-CAP system is split into $m = 6$ subcarriers, each of 4.26 GHz bandwidth while the single CAP system occupies 25 GHz bandwidth. It was found that a transmission speeds of 102.4 Gb/s and 100 Gb/s could be achieved for multi-CAP and CAP, respectively. This is not a significant gain in transmission speed; however a substantial improvement in dispersion and SNR performance, as well as a substantial reduction in computation complexity due to a reduction in sampling frequency per carrier, was also reported. In terms of computational complexity, as the order of m increases, the number of FIR filters increases by $2m$ in both the transmitter and receiver. If m is selected excessively high this can introduce additional computational complexity, which is undesirable. On the other hand, the literature has shown that increasing m results in a reduction of overall sampling frequency requirements, causing them to approach the Nyquist rate, meaning lower clock speeds can be used in the digital signal processors. Finally, although the pulse shaping filter required for m-CAP is more involved than that of OFDM, the IFFT/FFT required by OFDM is still a more complex operation than designing a pulse shaping filter for m-CAP. Moreover, such an m-CAP pulse shaping filter is physically realisable as demonstrated in the experiments presented in this paper.

Provided the system design process as described in this paper is followed and the pulse shaping filter correctly realised (having matched pulse shaping filters at the transmitter and receiver), we do not expect it to have any adverse effect on the system performance.

We believe that the proposed m-CAP system is an effective method for improving the bandwidth usage in VLC systems. However there have been no experimental or theoretical demonstrations of its suitability to date. Therefore in this work we propose to investigate a number of m-CAP systems with increasing number of subcarriers belonging to the set $m = \{2, 4, 6, 8, 10\}$, in comparison to the traditional, single-carrier CAP format. First we load every subcarrier in every system with binary phase-shift keying (BPSK) before transmission in order to establish the SNR/subcarrier before increasing the number of bits/symbol to the maximum allowed by our experimental system. We demonstrate that transmission speeds (spectral efficiencies) of 31.53 (4.85), 30.88 (4.75), 25.40 (3.90), 23.65 (3.60), 15.78 (2.40), 9.04 (1.40) Mb/s (b/s/Hz) can be achieved for $m = \{10, 8, 6, 4, 2, 1\}$, respectively.

This paper is organized as follows. In Section II the communications test setup and theoretical description of the m-CAP modulation format is discussed. Finally in Section III and IV the results are discussed and the conclusions are drawn, respectively.

II. m-CAP Test Setup

The test setup for our link is shown in Fig. 1 in the form of a schematic block diagram and picture of the experimental setup inset. A $2^{11} - 1$ pseudorandom binary seqeuence is generated for each subcarrier D_m where m is the subcarrier, before being mapped into the M_m-QAM modulation format, where $M = 2^k$ and k is the number of bits/symbol. In the first instance $k = 1$, as mentioned. The signal is upsampled before being split into the real and imaginary parts before filtering. The I_m and Q_m filters form a Hilbert pair. The impulse response of the filters are given as the product of a square root raised cosine (SRRC) filter and a cosine (real) or sine (imaginary) wave with frequency at least twice that of the pulse width of the SRRC filter. The roll-off factor of the SRRC is set to $\beta = 0.15$, as is consistent with the literature [15], [16]. The concept of impulse response generation is illustrated in Fig. 2 where the top half shows the filter impulse response for the real-valued upsampled QAM data (blue), SRRC impulse (red) and cosine (black); the bottom half shows the imaginary-valued upsampled QAM data filter impulse response (green), SRRC impulse (red) and sine (black). For higher subcarriers the frequency of the (co)sine wave is simply increased appropriately.

The output of each filter is real-valued and summed to form the time domain signal for transmission. The output signal $s(t)$ is given by [17]:

$$s(t) = \sum_{n=1}^{m} \left[A_I^n(t) \otimes f_I^n(t) - A_Q^n(t) \otimes f_Q^n(t) \right] \qquad (1)$$

where $\otimes$ denotes time-domain convolution, A_I^n and A_Q^n are the in-phase and quadrature M_m-QAM mapped symbols on the n^{th} subcarrier and f_I^n and f_Q^n are the in-phase and quadrature transmit filters of the n^{th} subcarrier, respectively. The impulse responses of the transmit filters are given by [17]:

$$f_I^m(t) = \left[\frac{\sin\left(\xi\left[1-\beta\right]\right) + 4\beta\frac{t}{T_s}\cos\left(\xi\left[1+\beta\right]\right)}{\xi\left[1-\left(4\beta\frac{t}{T_s}\right)^2\right]} \right] \cdot \sin\left(\pi\frac{t}{T_s}\left(2m-1\right)\left(1+\beta\right)\right) \qquad (2)$$

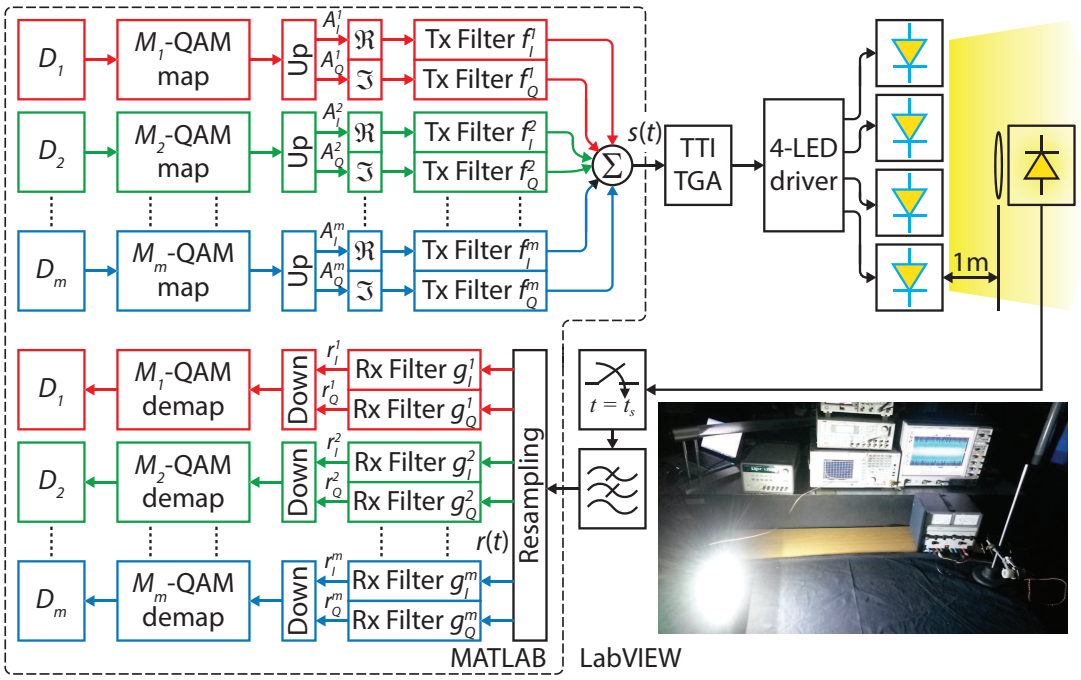

Fig. 1. Schematic block diagram of the system under test including a photograph inset; it should be noted that the Up block indicates up-sampling and the Down block indicates down-sampling

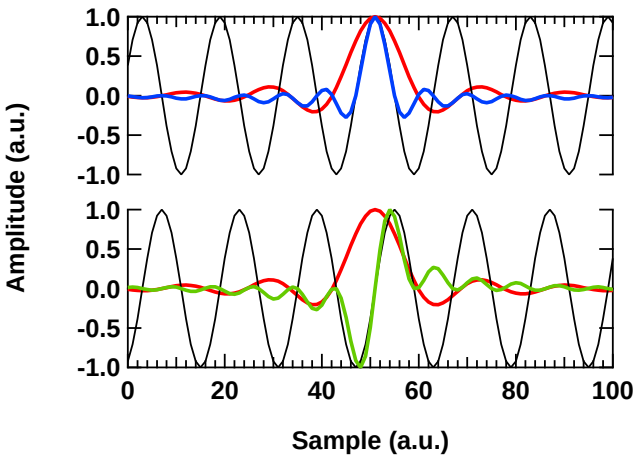

Fig. 2. (Top) shows the cosine carrier (black), SRRC impulse response (red) and overall in-phase filter impulse response (blue) for the first subcarrier of an m-CAP system; (bottom) shows the sine carrier (black), SRRC impulse (red) and quadrature filter impulse (green) for the same subcarrier

for the in-phase filter and the following for the quadrature filter, where T_s is the symbol duration and $\xi = \pi \frac{t}{T_s}$ [17]:

$$f_I^m(t) = \left[\frac{\sin\left(\xi\left[1-\beta\right]\right) + 4\beta\frac{t}{T_s}\cos\left(\xi\left[1+\beta\right]\right)}{\xi\left[1-\left(4\beta\frac{t}{T_s}\right)^2\right]} \right] \cdot \cos\left(\pi\frac{t}{T_s}\left(2m-1\right)\left(1+\beta\right)\right) \quad (3)$$

A TTI TGA12104 arbitrary waveform generator is selected due to its deep memory (up to 1 Mpoints) and high arbitrary clock frequency (up to 100 MHz). The signal frequency is given as the ratio of the length of the data sequence to the desired transmission frequency. Therefore in this work, due to the high length of the transmission sequences, the transmission bandwidth is limited to 6.5 MHz. On the other hand, the bandwidth of our Ce:YAG/GaN LEDs is 4.5 MHz, meaning an additional 2 MHz is required for communications and hence there is an out of band transmission, where high attenuation can be expected.

Thus with the 6.5 MHz bandwidth limitation imposed, the m-CAP system must be designed appropriately. The baud rates are set as follows; 6.50, 3.25, 1.625, 1.083, 0.8125 and 0.65 Mbaud for $m = \{1, 2, 4, 6, 8, 10\}$, respectively and this is illustrated in Fig. 3.

The arbitrary waveform generator is controlled by LabVIEW and feeds a custom transmission circuit that is detailed in [18]. The circuit is a current mirror with four arms that intensity modulates four individual Ce:YAG/GaN LEDs with the same signal. The LEDs are biased at 350 mA to ensure operation in the linear region (see Fig. 4 for the measured L-I-V curve).

This allows us to set the transmission distance at $\sim$1 m, which is substantially larger than in the majority of the experimentally tested VLC systems published in literature [1], [8], [19]. The light is focused onto the photodetector (OSD15-5T) using a 25 mm bi-convex lens with a focal distance of 25 mm. The photocurrent is passed through an Analog Devices AD8015 differential transimpedance amplifier before both of the differential channels are digitized by an Agilent DSO9254A real time oscilloscope.

After capture, the signal is processed offline in MATLAB starting with a 4$^{\text{th}}$ order low pass filter with cut-off frequency set to 6.5 MHz to remove out of band noise. The dominant noise source in this system is expected to be the shot and

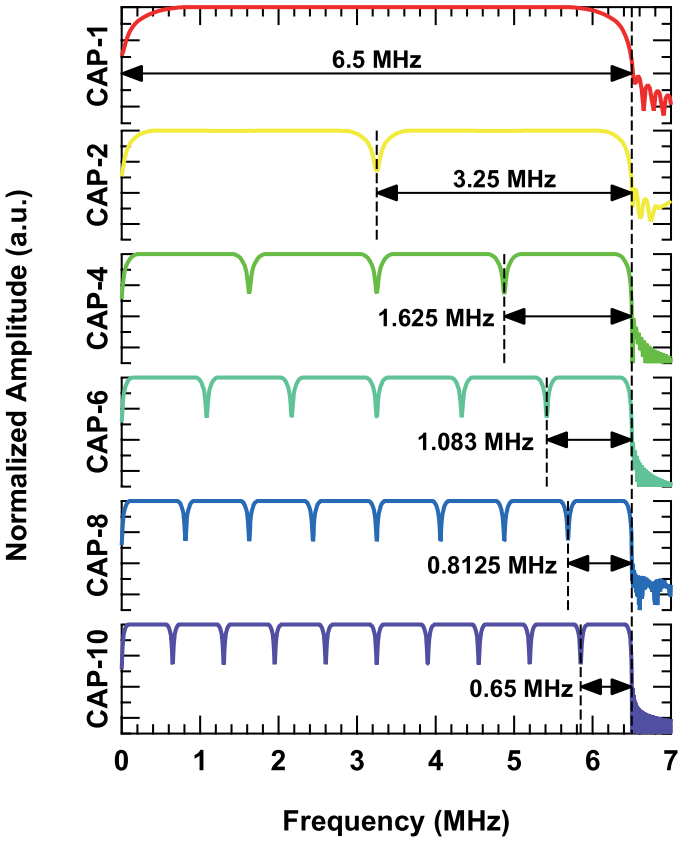

Fig. 3. Ideal frequency responses and bandwidth requirements for different orders of m

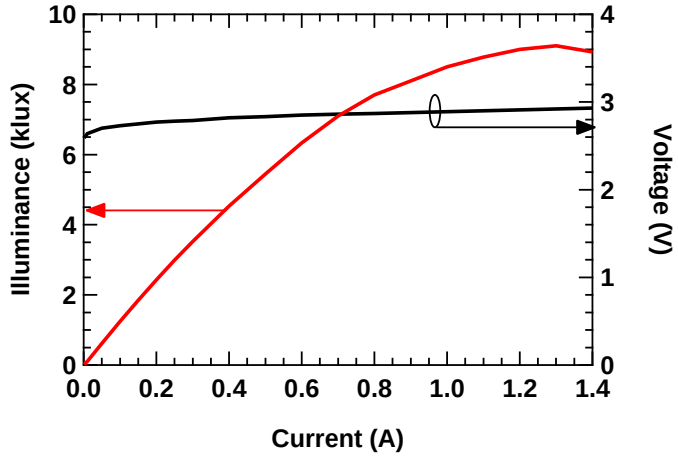

Fig. 4. Measured L-I-V curves of a single Ce:YAG/GaN LED used in this work

thermal noise introduced by the receiver electronics which can be modelled as additive white Gaussian noise sources [12], as opposed to ambient noise or noise induced by clipping from the LED L-I-V response. After low pass filtering, the signal is resampled to match that of a reference version of the transmitted signal and passed through the time-reversed in-phase and quadrature receiver filters g_I and g_Q, which are matched to the corresponding transmit filter so that $g_I^m(t) = f_I^m(-t)$ and $g_Q^m(t) = f_Q^m(-t)$. The received in-phase and quadrature signals are given as follows [17]:

$$r_I^m(t) = r(t) \otimes g_I^m(t) \tag{4}$$

for the in-phase receiver matched filter and

$$r_Q^m(t) = r(t) \otimes g_Q^m(t) \tag{5}$$

for the quadrature receiver matched filter, where $r(t)$ is the discrete time digitized signal after resampling.

In the first instance, BPSK is transmitted in order to gain an estimate of the SNR available in each subcarrier as in [19]. The SNR is estimated as the square of the root mean square error vector magnitude (EVM) measured from the received BPSK constellation as follows [20]:

$$\text{SNR} = \frac{1}{\text{EVM}^2} \tag{6}$$

The received and measured SNR values and assigned M_m-QAM modulation orders are illustrated in Fig. 5 and Fig. 6, respectively. Although at least 10^5 bits are captured during the measurements, the BER target was set at 10^{-3}, in order to provide a small error allowance in consideration of the forward error correction (FEC) 7% and 20% BER limits of 3.8×10^{-3} and 2×10^{-2}, respectively [21]. Thus, several theoretical SNR thresholds emerge that dictate the maximum number of bits-per-symbol-per-subcarrier, which are shown as dashed lines in Fig. 5. The exact values can easily be found in the literature [21] as follows; $SNR_{threshold} = \{6.7, 9.5, 10.5, 13.5, 14.7, 18\}$ dB for $k = \{2, 3, 4, 5, 6, 7\}$ bits/symbol, respectively at a BER of 10^{-3}. From Fig. 5 it is inferrable that for $m > 1$ the number of bits-per-symbol can be optimized from the measured SNRs as shown in Fig. 6, which states the allocation for each m-CAP system. The maximum SNR value measured is 23.22 dB for the 4$^{\text{th}}$ subcarrier of 10-CAP. On the other hand, for $m = 1$ the threshold for 4-QAM is not met. Instead of selected BPSK for the 1-CAP modulation format we decided that it was advantageous to persist with 4-QAM at the cost of a higher BER ($\sim 10^{-2}$), which is still beneath the 20% FEC limit.

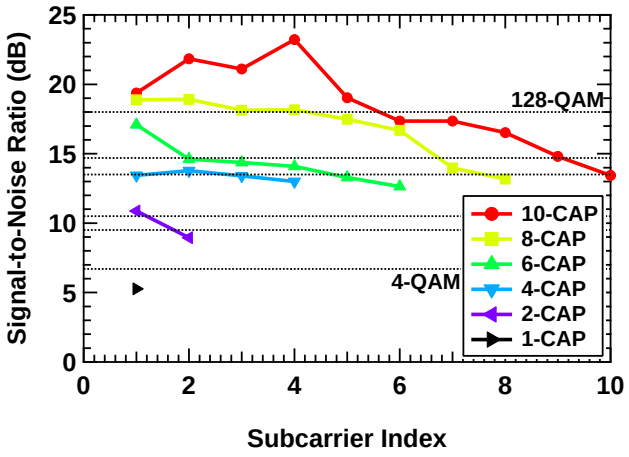

Fig. 5. Measured SNR from the BPSK tests for each m-CAP system tested; also shown are the SNR thresholds

The m-CAP signals optimized with the appropriate number of bits-per-symbol-per-subcarrier are subsequently loaded into the TTI TGA12104 and the same routine occurs. There have been reports of equalization in the literature before de-mapping

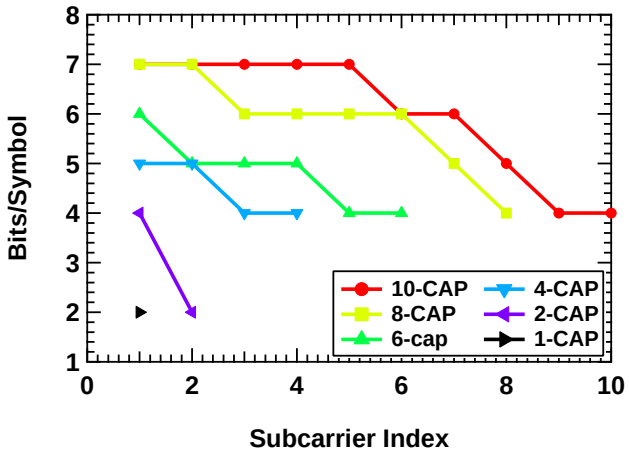

Fig. 6. The assigned number of bits-per-symbol for each value of m-CAP

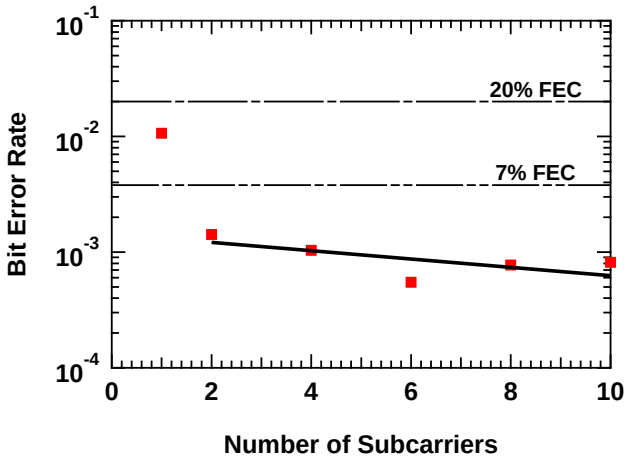

Fig. 7. The measured BER performance for every value of m-CAP; showing the BER for $m = 1$ ($\sim 10^{-2}$) and for $m > 1$ ($\sim 10^{-3}$) as expected

from the M_m-QAM constellation, including the use of analogue [10] and digital [22] frequency domain equalizers, the constant multi-modulus [17], [23], least mean squares [24] and k-means [15] algorithms and decision feedback equalization [25], [26], 26]. In this work we do not consider an equalizer because we would like to demonstrate the raw improvement in spectral efficiency with increasing order of m. Further, in an m-CAP system with a high m, an individual equalizer would be required for every subcarrier, drastically increasing the computational complexity and surrendering some of the advantages of CAP over OFDM and single-carrier QAM systems.

The received signal is then downsampled and de-mapped from the M_m-QAM constellation to give an estimate of the transmitted symbols. The estimates are compared with the actual transmitted symbols to provide a symbol-by-symbol BER performance characterisation for each value of m.

III. Results

The results will be discussed as follows. The BER performance of each m-CAP system is shown in Fig. 7, which also highlights the FEC limits of 3.8×10^{-3} (7%) and 2×10^{-2} (20%). Following a discussion of the overall BER performance for each system and considering the 6.5 MHz bandwidth occupancy, the available transmission speed and spectral efficiency will be discussed for every m-CAP system in descending order. The BER is calculated by aggregating the individual BERs from each subcarrier in the same manner as the overall transmission speed is calculated as the sum of the total capacity from each subcarrier.

Overall, for $m > 1$ the 7% FEC limit is comfortably met as expected due to the BER targets set, shown with a linear fit in Fig. 7, excluding $m = 1$. The aggregated BER for each m-CAP system is approximately 10^{-3} as expected, indicating the correct functionality of the system. For higher orders of m (i.e. $m = 10$) it can be seen that the measured SNR is comfortably above the threshold for 128-QAM, yet the BER performance is close to the 10^{-3} threshold (exact BER $= 8.17 \times 10^{-4}$). The reason is because a high number of bit errors are introduced by the high subcarriers, which are very close to the threshold limits for the target BER. Further, it is clear that the worst performance occurs for the 1-CAP system, which offers a BER of $\sim 10^{-2}$, failing to meet the 7% FEC limit as expected but comfortably within the 20% FEC limit. This is not a fatal problem for 1-CAP; however it does mean a significantly larger overhead of redundant symbols and a further reduction in spectral efficiency in comparison to the other systems, especially considering that 4-QAM is used as the modulation order.

Further insight into the system performance can be gained by analysing the EVM-per-subcarrier for each m-CAP system as is illustrated in Fig. 8, which does not include the EVM_{RMS} result for 1-CAP. The reason for this is because 1-CAP achieved an EVM result of 43.32% and caused a severe reduction in resolution of the y-axis, distorting the remaining data. Clearly the EVM results follow a similar trend of a reduction in EVM with an increasing order of m. Recalling that the high-index subcarriers are carried at higher frequencies than the low-index subcarriers, the increased EVM is heavily dependent on the modulation bandwidth of the system (4.5 MHz). Subcarriers outside of the bandwidth experience a higher level of attenuation due to the characteristic low pass frequency response and thus the EVM increases substantially due to the reduced signal power.

A discussion of the individual m-CAP performances will commence in the next subsections.

A. 10-CAP

The received and normalized electrical spectra for 10-CAP is shown in Fig. 9 with constellations for the 1st (red), 6th (blue) and 10th (green) subcarriers inset as highlighted in their respective colours. The EVM_{RMS} values for the three constellations shown are 4.1741%, 7.7326% and 15.666% for the 1st, 6th and 10th subcarriers, respectively.

The gross transmission speed that can be achieved using the 10-CAP system at a BER of 10^{-3} is 33.9 Mb/s. After removal of the 7% FEC overhead, this corresponds to a net transmission speed of 31.53 Mb/s. It should be noted that the point of this paper is not to set a world record transmission

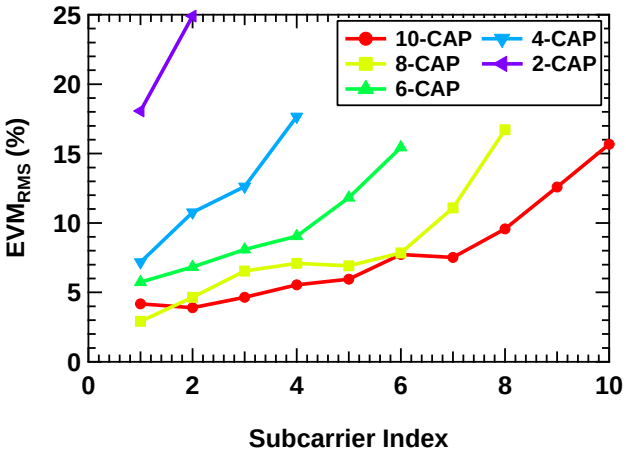

Fig. 8. The measured EVM for each subcarrier for every version of m-CAP tested; showing a clear improvement with increasing m

speed but to demonstrate the gain that can be achieved using the proposed m-CAP system. Recalling that the maximum bandwidth allowed by the TGA12104 is 6.5 MHz, this was adopted as the transmission bandwidth, corresponding to a spectral efficiency of 4.85 b/s/Hz; the highest reported in this work. To the best of the authors collective knowledge, this is the highest spectral efficiency reported in any VLC system at the 1 m distance considered. Other systems have reported higher spectral efficiencies; for example 6.25 b/s/Hz was demonstrated in [19], however the link distance had to be severely reduced to just 0.05 m in order to do achieve this, a reduction of twenty-fold in comparison to this work. We anticipate with a smaller distance the spectral efficiency we report could be improved beyond 6.25 b/s/Hz; due to the additional optical power that would be absorbed by the photodetector. This would benefit not only the low-index subcarriers but more importantly the high-index subcarriers where the number of bits-per-symbol was severely limited by noise. This is best demonstrated by examining the eye diagrams of the 1st and 10th subcarriers at the receiver.

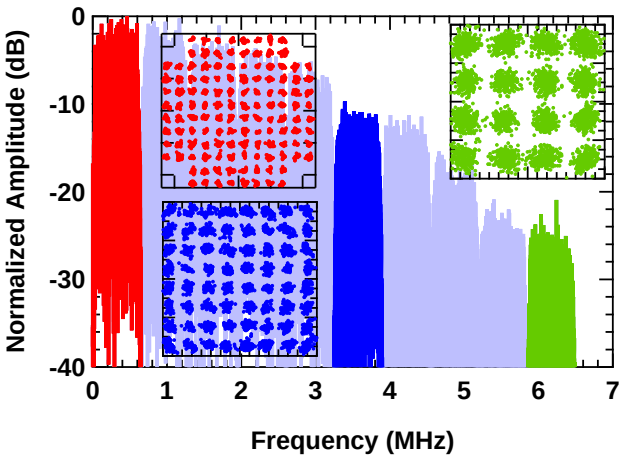

Fig. 9. The measured electrical spectrum of the 10-CAP system with 6.5 MHz bandwidth showing clear and increasing attenuation with every additional subcarrier; inset are the constellations for the highlighted subcarriers

Only the in-phase signals are shown (equally we could have

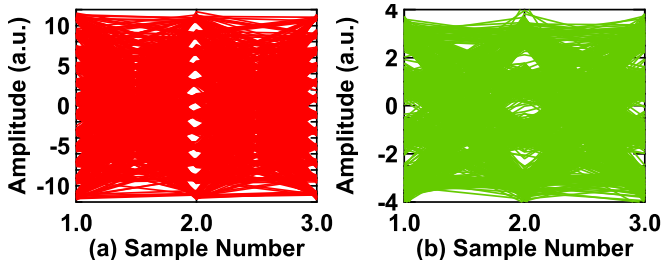

Fig. 10. Eye diagram of 10-CAP down-sampled data for (a) subcarrier 1 and (b) subcarrier 10; clearly subcarrier 1 shows a significantly improved SNR over subcarrier 10 due to the clean eye opening (note the different y-axis scales)

shown the quadrature) after being down-sampled. The two eye diagrams are shown in Fig. 10(a) and (b), respectively, where the difference in SNR is clear. With a shorter distance the SNR of both would improve and thus more bits-per-symbol could be added and a higher spectral efficiency achieved.

B. 8-CAP

The gross transmission speed that can be supported using the 8-CAP system is slightly reduced to 33.2 Mb/s in comparison to the 33.9 Mb/s available in 10-CAP; a reduction of 0.7 Mb/s. After removal of the overhead the net transmission speed available is 30.88 Mb/s, ∼0.65 Mb/s less than for 10-CAP and therefore a slight reduction in spectral efficiency to 4.75 b/s/Hz, or a 0.1 b/s/Hz reduction, which could be considered negligible for the current system. We suggest this because if the transmission speed is approximately equal, the system complexity can be reduced by omitting the 9th and 10th subcarriers at the transmitter and receiver at the cost of 0.65 Mb/s. Recalling that the most expensive filters computationally are the ones that require the highest sampling frequencies this could be classed as a significant advantage.

C. 6-CAP

For 6-CAP the overall transmission speed is 27.3 Mb/s before overhead removal; a large reduction over 8-CAP and 10-CAP of at least 5.9 Mb/s. After overhead removal the data rate drops to 25.4 Mb/s with a spectral efficiency of 3.9 b/s/Hz. The severe reduction in capacity for 6-CAP in comparison to the previous two systems is attributed to the wider subcarrier bandwidth of 1.083 MHz, which is more prone to attenuation that the previous bands, which were both $\leq$ 0.8125 MHz. This causes a significant reduction in SNR (as can be referred to in Fig. 5), meaning a lower allocation of bits-per-symbol (Fig. 6) and a higher EVM (Fig. 8). It can be noted from Fig. 5, 6 and 7 that both the profiles of 8-CAP and 10-CAP are very similar, when considering a frequency normalized case, thus explaining their very similar performances and their additional performance over 6-CAP.

D. 4-CAP and 2-CAP

4-CAP offers a gross (net) throughput of 25.40 (23.65) Mb/s, a further drop of 1.90 (1.75) Mb/s in comparison to 6-CAP and a large drop of 8.50 (7.88) Mb/s

in comparison to 10-CAP and the spectral efficiency is reduced to 3.6 b/s/Hz. For the 2-CAP system, there is a substantial drop in gross (net) throughput to ∼17 (15.78) Mb/s. This is a substantial drop in comparison to 4-CAP and a drop of around 50% when considering the transmission speeds of 10-CAP and 8-CAP are slightly over 30 Mb/s. This can be attributed once more to the bandwidth of the subcarriers; for $m = \{4, 6, 8, 10\}$ the bandwidth sizes vary by a fraction of a single MHz, meaning that the baud rate for each constellation must increase in order to maintain the overall transmission speed and hence there is a slight dip with decreasing m. However for $m = 2$, the bandwidth doubles in comparison to $m = 4$ indicating a substantially larger attenuation. This is reflected in the electrical spectrum of the 2-CAP signal (Fig. 11), which, for the first subcarrier, shows attenuation of ∼8–10 dB and, for the second subcarrier, ∼10–12 dB.

When comparing with 10-CAP (Fig. 9), there is no obvious attenuation in any of the subcarriers until the 9th and 10th subcarriers, which show ∼1 dB each. The spectral efficiency of 2-CAP is 2.4 b/s/Hz, confirming the substantial drop in efficiency.

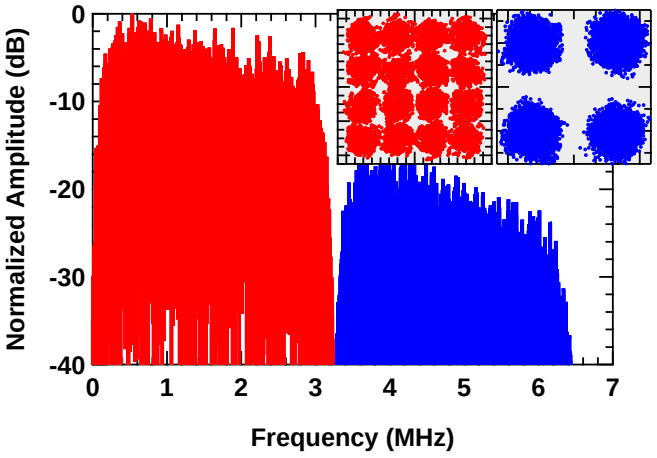

Fig. 11. Measured electrical spectrum of 2-CAP, showing much higher attenuation per subcarrier than previous spectra; thus the EVM of the inset subcarriers is severely reduced

E. 1-CAP

The conventional 1-CAP system can support a gross data rate of 11.3 Mb/s. Recalling that the BER of the 1-CAP system is $\sim 10^{-2}$ it is not possible to use a 7% FEC in this case. Thus, the 20% FEC must be used here, reducing the overall transmission speed to 9.04 Mb/s, thus dropping beneath 10 Mb/s for the first time. In comparison to 10-CAP this is a drop of > 20 Mb/s, while in comparison to 2-CAP a drop of ∼6 Mb/s is reported. The spectral efficiency drops to 1.4 b/s/Hz; the lowest efficiency reported here and a massive ∼3.5 times smaller than 10-CAP and 8-CAP. Just as reported with 2-CAP, this is attributed to the large attenuation suffered due to out-of-band transmission, refer to the electrical spectrum in Fig. 12 which shows 10–20 dB attenuation.

Finally, in Fig. 13 we summarize the reported results into a graph that shows the net transmission speed and spectral efficiency simultaneously. The data corresponds to both axes. It is possible to notice that the data follows an exponential trend and hence we fitted the curve to the available net transmission speed with the following equation:

$$R_b = 33.486 - 24.026 \exp\left(\frac{1-m}{3.6615}\right) \tag{7}$$

where R_b is the net transmission speed (Mb/s). As an exponential fit is required and not a linear fit, this implies asymptotic behaviour where at a certain point, increasing the number of subcarriers will not provide any improvement but will introduce additional computational complexity. We propose to theoretically investigate this in our future work in order to derive the upper bounds for the capacity of the m-CAP modulation format for VLC systems.

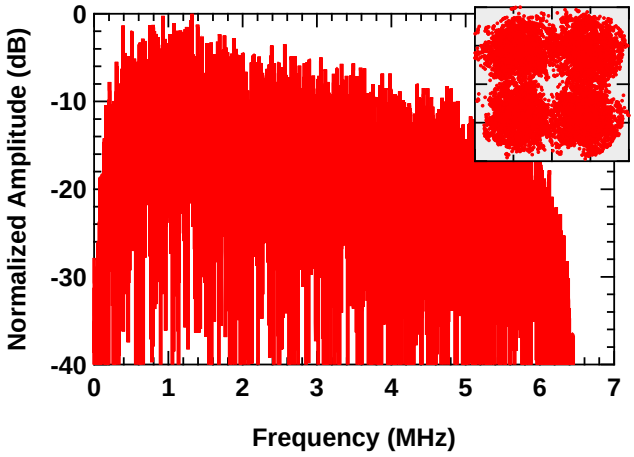

Fig. 12. Measured electrical spectrum for 1-CAP with 4-QAM constellation inset

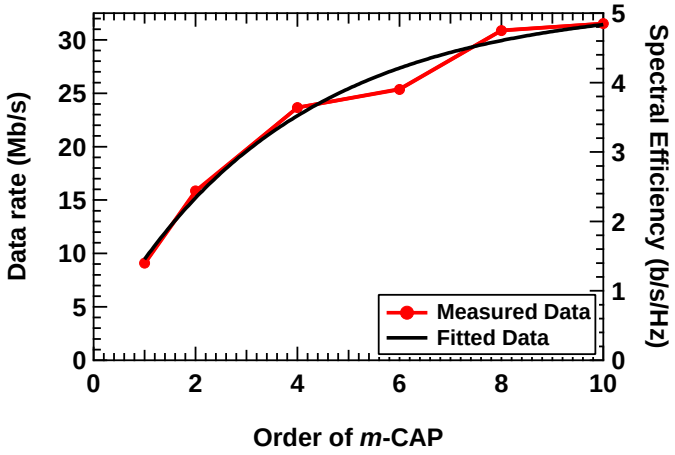

Fig. 13. Measured throughput and spectral efficiency for each order of m-CAP with exponential fitting curve implying an eventual asymptotic behaviour

IV. Conclusion

In this paper we have experimentally demonstrated an m-CAP system for VLC for the first time considering a fixed bandwidth of 6.5 MHz, where m is the number of subcarriers under consideration and belongs to the set $m =$

$\{10, 8, 6, 4, 2, 1\}$. We observed that for a higher number of subcarriers, a higher throughput could be supported, up to $\sim$31.5 Mb/s with a spectral efficiency of 4.85 b/s/Hz. Reducing the number of subcarriers results in a lower throughput and spectral efficiency due to the wider bandwidths of the subcarriers, which are more prone to high frequency attenuation in the first order low-pass VLC systems.

ACKNOWLEDGEMENTS

P. A. Haigh and A. Burton acknowledged financial support from Northumbria University.

P. A. Haigh also acknowledges James Thomas Steven Savage, University of Bristol, for providing the platform to perform several of the measurements.

This work was also supported by the EU COST Action IC1101.

REFERENCES

[1] H. Le Minh, D. O'Brien, G. Faulkner, Z. Lubin, L. Kyungwoo, J. Daekwang, O. YunJe, and W. Eun Tae, "100-Mb/s NRZ visible light communications using a postequalized white LED," *IEEE Photonics Technology Letters*, vol. 21, no. 15, pp. 1063–1065, 2009.

[2] L. Grobe, A. Paraskevopoulos, J. Hilt, D. Schulz, F. Lassak, F. Hartlieb, C. Kottke, V. Jungnickel, and K. D. Langer, "High-speed visible light communication systems," *IEEE Communications Magazine*, vol. 51, no. 12, pp. 60–66, 2013.

[3] P. A. Haigh, Z. Ghassemlooy, S. Rajbhandari, I. Papakonstantinou, and W. Popoola, "Visible light communications: 170 Mb/s using an artificial neural network equalizer in a low bandwidth white light configuration," *Journal of Lightwave Technology*, vol. 32, no. 9, pp. 1807–1813, 2014.

[4] D. S. Lee, X. Gao, S. Guo, D. Kopp, P. Fay, and T. Palacios, "300-GHz InAlN/GaN HEMTs with InGaN back barrier," *IEEE Electron Device Letters*, vol. 32, no. 11, pp. 1525–1527, 2011.

[5] J. Grubor, S. C. J. Lee, K.-D. Langer, T. Koonen, and J. W. Walewski, "Wireless high-speed data transmission with phosphorescent white-light LEDs," *ECOC 2007*, 2007.

[6] Z. Ghassemlooy, W. Popoola, and S. Rajbhandari, *Optical Wireless Communications: System and Channel Modelling*. CRC PressINC, 2012.

[7] W. O. Popoola and H. Haas, "Demonstration of the merit and limitation of generalised space shift keying for indoor visible light communications," *Journal of Lightwave Technology*, vol. 32, no. 10, pp. 1960–1965, 2014.

[8] G. Cossu, A. M. Khalid, P. Choudhury, R. Corsini, and E. Ciaramella, "3.4 Gbit/s visible optical wireless transmission based on RGB LED," *Opt Express*, vol. 20, no. 26, pp. B501–6.

[9] D. Bykhovsky and S. Arnon, "An experimental comparison of different bit-and-power-allocation algorithms for DCO-OFDM," *Journal of Lightwave Technology*, vol. 32, no. 8, pp. 1559–1564, 2014.

[10] F. M. Wu, C. T. Lin, C. C. Wei, C. W. Chen, Z. Y. Chen, H. T. Huang, and S. Chi, "Performance comparison of OFDM signal and CAP signal over high capacity RGB-LED-based WDM visible light communication," *IEEE Photonics Journal*, vol. 5, no. 4, pp. 7 901 507–7 901 507, 2013.

[11] A. F. Shalash and K. K. Parhi, "Multidimensional carrierless AM/PM systems for digital subscriber loops," *IEEE Transactions on Communications*, vol. 47, no. 11, pp. 1655–1667, 1999.

[12] J. Kahn and J. Barry, "Wireless infrared communications," *Proceedings of the IEEE*, vol. 85, no. 2, pp. 265–298, 1997.

[13] H. Le Minh, D. O'Brien, G. Faulkner, L. Zeng, K. Lee, D. Jung, and Y. Oh, "80 Mbit/s visible light communications using pre-equalized white LED," in *34th European Conference on Optical Communication, 2008*. IEEE, 2008, Conference Proceedings, pp. 1–2.

[14] P. A. Haigh, Z. Ghassemlooy, H. L. Minh, S. Rajbhandari, F. Arca, S. F. Tedde, O. Hayden, and I. Papakonstantinou, "Exploiting equalization techniques for improving data rates in organic optoelectronic devices for visible light communications," *Journal of Lightwave Technology*, vol. 30, no. 19, pp. 3081–3088, 2012.

[15] M. I. Olmedo, Z. Tianjian, J. B. Jensen, Z. Qiwen, X. Xiaogeng, S. Popov, and I. T. Monroy, "Multiband carrierless amplitude phase modulation for high capacity optical data links," *Journal of Lightwave Technology*, vol. 32, no. 4, pp. 798–804, 2014.

[16] M. Wieckowski, J. B. Jensen, I. Tafur Monroy, J. Siuzdak, and J. Turkiewicz, "300 Mbps transmission with 4.6 bit/s/Hz spectral efficiency over 50 m PMMA POF link using RC-LED and multi-level carrierless amplitude phase modulation," in *National Fiber Optic Engineers Conference*. Optical Society of America, Conference Proceedings, p. NTuB8.

[17] J. Zhang, J. Yu, F. Li, N. Chi, Z. Dong, and X. Li, "$11 \times 5 \times 9.3$ gb/s WDM-CAP-PON based on optical single-side band multi-level multi-band carrier-less amplitude and phase modulation with direct detection," *Optics express*, vol. 21, no. 16, pp. 18 842–18 848, 2013.

[18] A. Burton, E. Bentley, H. Le Minh, Z. Ghassemlooy, N. Aslam, and S.-K. Liaw, "Experimental demonstration of a 10BASE-T ethernet visible light communications system using white phosphor light-emitting diodes," *IET Circuits, Devices & Systems*, vol. 8, no. 4, 2014.

[19] D. Tsonev, H. Chun, S. Rajbhandari, J. McKendry, S. Videv, E. Gu, M. Haji, S. Watson, A. Kelly, G. Faulkner, M. Dawson, H. Haas, and D. O'Brien, "A 3-Gb/s Single-LED OFDM-based wireless VLC link using a gallium nitride μled," *IEEE Photonics Technology Letters*, vol. PP, no. 99, pp. 1–1, 2014.

[20] R. A. Shafik, S. Rahman, and R. Islam, "On the extended relationships among evm, ber and snr as performance metrics," in *International Conference on Electrical and Computer Engineering, 2006*, 2006, Conference Proceedings, pp. 408–411.

[21] J. Proakis, *Digital Communications*. New York: McGraw-Hill, 2004.

[22] R. Rodes, M. Wieckowski, T. T. Pham, J. B. Jensen, J. Turkiewicz, J. Siuzdak, and I. T. Monroy, "Carrierless amplitude phase modulation of VCSEL with 4 bit/s/hz spectral efficiency for use in WDM-PON," *Optics express*, vol. 19, no. 27, pp. 26 551–26 556, 2011.

[23] L. Tao, Y. Wang, Y. Gao, A. P. T. Lau, N. Chi, and C. Lu, "Experimental demonstration of 10 Gb/s multi-level carrier-less amplitude and phase modulation for short range optical communication systems," *Optics Express*, vol. 21, no. 5, pp. 6459–6465, 2013.

[24] L. Tao, Y. Wang, Y. Gao, A. P. T. Lau, N. Chi, and L. Chao, "40 Gb/s CAP32 system with DD-LMS equalizer for short reach optical transmissions," *IEEE Photonics Technology Letters*, vol. 25, no. 23, pp. 2346–2349, 2013.

[25] J. Wei, D. Cunningham, R. Penty, and I. White, "Study of 100 gigabit ethernet using carrierless amplitude/phase modulation and optical OFDM," *Journal of Lightwave Technology*, vol. 31, no. 9, pp. 1367–1373, 2013.

[26] J. Wei, L. Geng, D. G. Cunningham, R. V. Penty, and I. White, "100 gigabit ethernet transmission enabled by carrierless amplitude and phase modulation using QAM receivers," in *Optical Fiber Communication Conference*. Optical Society of America, Conference Proceedings, p. OW4A. 5.